

Exploring wintertime regional haze in Northeast China: role of coal and biomass burning

Zhang et al.,

We are grateful for Referee#1's comments. These comments are all valuable and helpful for improving our paper. We answered the comments carefully and have made corrections in the submitted manuscript. The corrections and the responses are as following:

In the revised manuscript and supplement, the red color was marked as the revised places.

General comment

1. I have a major concern about the sampling. The authors should explain whether these 2 haze types within such a short period (1 week) could represent the typical haze type in NE China. What is the sampling strategy behind? What are possible limitations? I suggest the author include non-haze periods for comparisons. Without the detailed discussion, one may not agree that these 2 haze types could represent regional haze formation in NE China. In addition, only weak evidence was present to explain the formation mechanism. This should be clarified carefully.

Reply: We thanked the reviewer and carefully considered the comments. Firstly, we added the comparisons on chemical compositions during the haze period and non-haze period (clean day) (Figure 2). Here we selected one urban site and one mountain site that cover the regional scale in Northeast China. In fact, we conducted the field campaign about two weeks instead of one week. Here we only selected these two typical haze events as the case. As the referee's concern, we added another one week data in the supplemental materials (Figure S2). But in the main context, we still focused on these two haze events because the data is interesting. In the discussion section, we compared our results with previous studies through radar observation and model simulation, indicating the representativeness of these two haze events.

We added three figures of concentration-weighted trajectory (CWT) plots of PM_{2.5} in Figures S5b-d, which indicated the geographic origins of haze pollutants. We also added O₃ concentrations in Figure S6d, which showed quite low levels of O₃ during the heavy Haze-I event. Moreover, we added some marks in Figure 6 to indicate the phases and

mixing states of haze particles. These results well contributed to explain the haze formation mechanism.

P6 L130-132: “In this study, we conducted a field experiment in the south part of Northeast China from 25 October to 6 November 2016. Two contrasting regional heavy haze events occurred during 31 October-5 November 2016.”

P11 L250-251: “The concentrations of PM_{2.5} and its chemical compositions during the sampling period were showed in Figure S2.”

P11-12 L269-274: “The average mass concentrations of OM, EC, and secondary inorganic ions (i.e., SO₄²⁻, NO₃⁻, and NH₄⁺) in PM_{2.5} increased from 11 µg/m³, 3.0 µg/m³, and 6 µg/m³ during the clean day to 45 µg/m³, 4.3 µg/m³, and 24 µg/m³ during the moderate Haze-I event at the urban site and from 9 µg/m³, 0.9 µg/m³, and 3 µg/m³ to 39 µg/m³, 2.7 µg/m³, and 20 µg/m³ at the mountain site, respectively (Figures 2b-c).”

P17 L436-438: “Figures S5c-d further indicate that compared with transport from Beijing-Tianjin-Hebei region, local secondary transformation was one major factor to cause the heavy Haze-I formation.”

P18 L441-449: “Because of low O₃ level at 12 ppb (Figure S6d) and thick haze layer weakening solar radiation (Zhao et al., 2013; Zheng et al., 2015) during the heavy Haze-I event, photochemical activity should be ignored in air and heterogeneous chemical reactions on particle surfaces can be considered as major pathways in the formation of sulfates and nitrates from SO₂ and NO_x whenever RH exceeds 70% (Sun et al., 2018; Wang et al., 2016a; Wu et al., 2018). Here, TEM observations did show that the heavy Haze-I particles were wet aerosols and presented S-rich coating on primary OM, soot, or fly ash/metal particles at 73-80% of RH (Figures 6c-d and S4c-d).”

P19 L483-492: “The above formation mechanisms of two haze events are similar to previous studies through radar observation (Zhong et al., 2019) and model simulation (Yang et al., 2017). These studies indicated that adverse meteorological conditions (e.g., low wind speed and high RH) and high-intensity emissions of residential heating and biomass burning mainly contributed to the haze formation in Northeast China in winter. In addition, our previous study suggested that heterogeneous reactions were one major factor for regional winter haze evolution in Northeast China (Zhang et al., 2017).

Therefore, we confirmed these two continuous haze events as one typical haze pollution occurring in Northeast China during winter.”

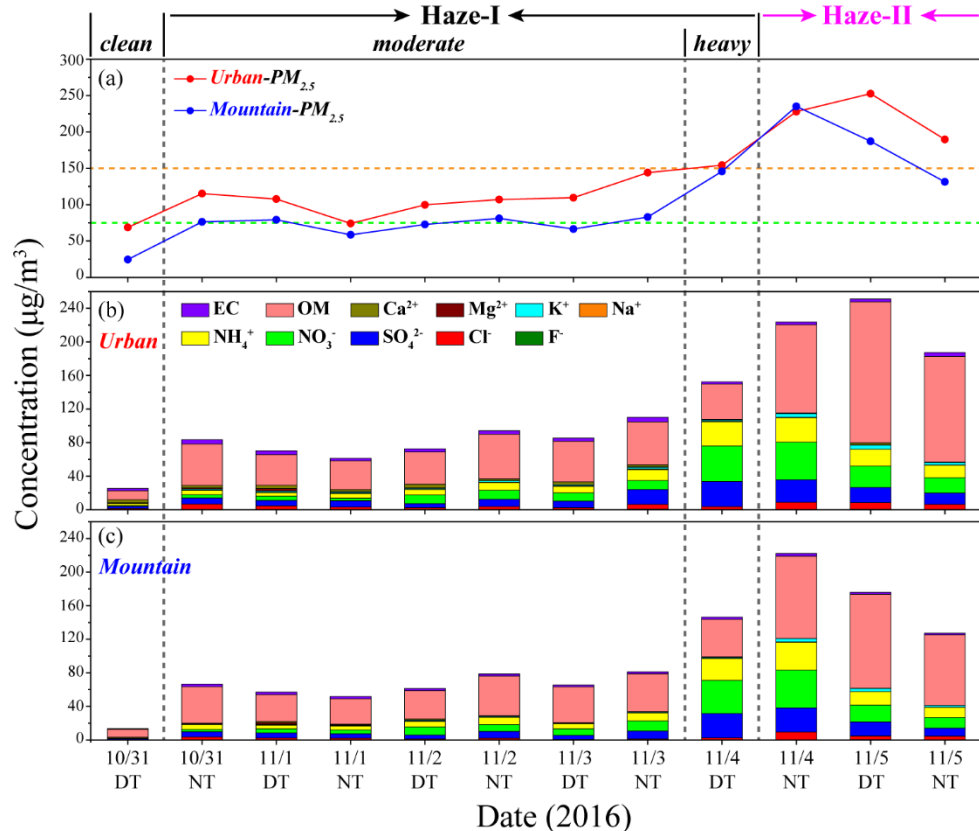


Figure 2. Variation in the concentrations of PM_{2.5}, organic matter (OM), elemental carbon (EC), and water-soluble ions (i.e., Ca²⁺, Mg²⁺, K⁺, Na⁺, NH₄⁺, NO₃⁻, SO₄²⁻, Cl⁻, and F⁻) at the urban and mountain sites from daytime (DT) on 31 October to nighttime (NT) on 5 November 2016: **(a)** PM_{2.5}; **(b-c)** OM, EC, and water-soluble ions. Two regional haze episodes (Haze-I: 31 NT October-4 DT November; Haze-II: 4 NT-5 NT November) were identified.

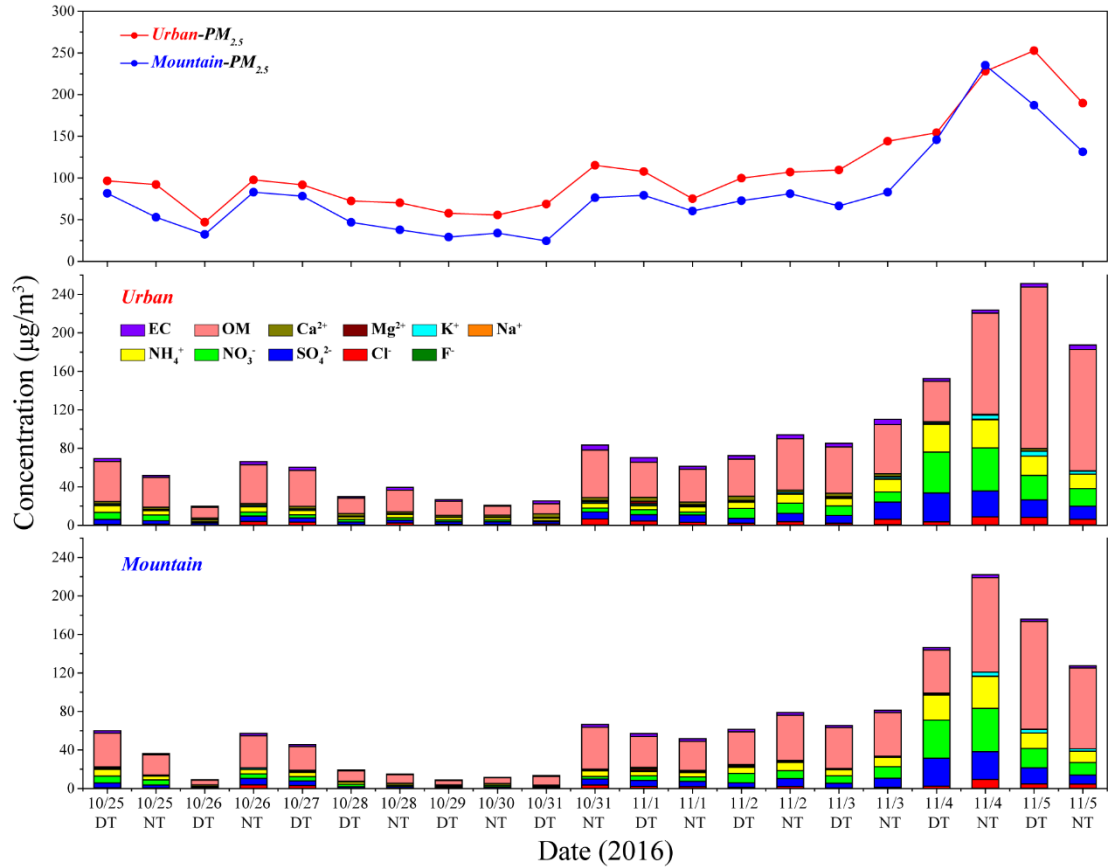


Figure S2. Time series of mass concentrations of $\text{PM}_{2.5}$ and its chemical compositions at the urban and mountain sites during the sampling period.

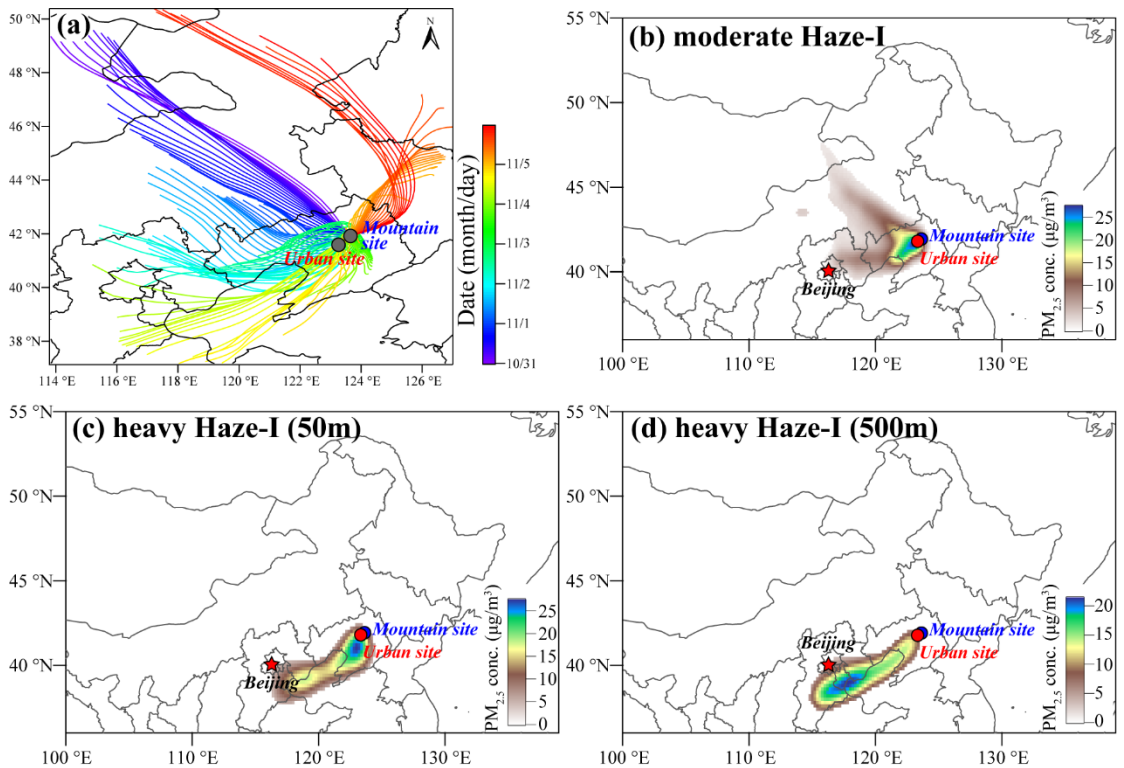


Figure S5. (a) 24-h air mass backward trajectories on 500 m height before arriving at Shenyang during 31 October-5 November. Concentration-weighted trajectory (CWT) plots of PM_{2.5} at the urban and mountain sites during the Haze-I event: (b) moderate Haze-I on 500 m height; (c-d) heavy Haze-I on 50 m and 500 m heights.

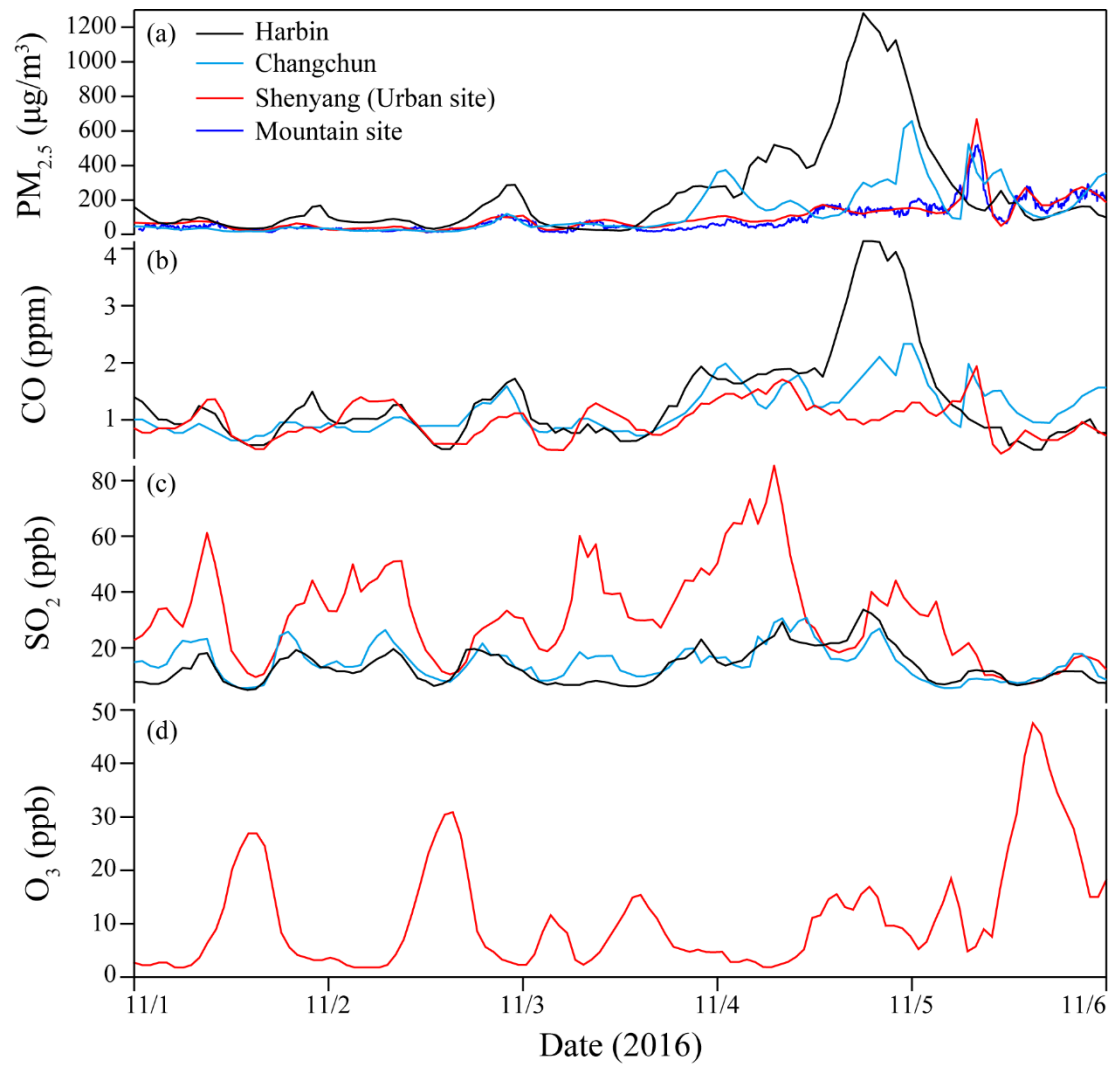


Figure S6. Time series of PM_{2.5} and three trace gases (i.e., CO, SO₂, and O₃) in Harbin city, Changchun city, Shenyang city (the urban site), and the mountain site from 1 to 5 November 2016: (a) PM_{2.5}; (b) CO; (c) SO₂; (d) O₃. These data have been obtained from China's Air Quality Online Monitoring and Analysis Platform, except for the PM_{2.5} at the mountain site.

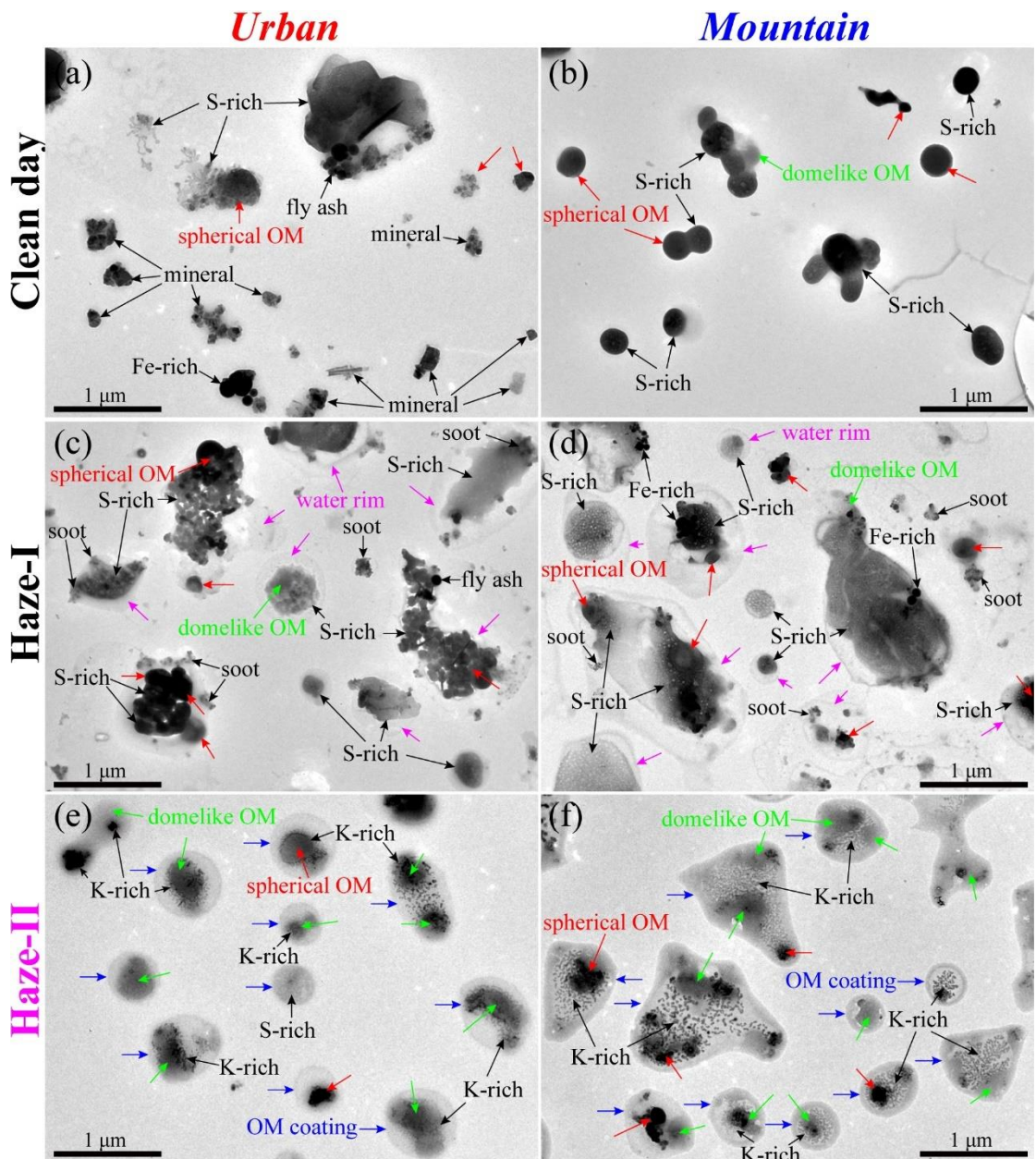


Figure 6. Typical TEM images of individual aerosol particles at low magnification at the urban and mountain sites: **(a-b)** clean day; **(c-d)** Haze-I; **(e-f)** Haze-II. The red, green, blue, and pink arrows represent spherical OM, domelike OM, OM coating, and water rim, respectively.

2. Abstract: Lines 20-21: this may be not true.

Reply: We revised this sentence as follows.

P2 L20-21: “Northeast China faces serious problem on regional haze during the heating period of half a year.”

3. Line 23: delete the expression “for the first time” in the abstract.

Reply: We deleted “for the first time”.

P2 L23: “Here, we integrated bulk chemical measurements with single particle analysis...”

4. Methods: PM_{2.5} mass: quartz filter was not a good option. So this should be compared with the nearby monitoring stations.

Reply: Thanks. We added Table S1 to compare our PM_{2.5} data with the data reported from nearby monitoring station.

P7-8 L160-164: “In addition, we recorded the PM_{2.5} concentrations reported by nearby monitoring station during the sampling period and further compared them with our PM_{2.5} data as shown in Table S1. Although there is a 7-14% deviation between these two datasets, the variations of PM_{2.5} concentrations are same (Table S1). Therefore, our PM_{2.5} data can represent the condition of haze pollution during the sampling period.”

Table S1. Comparison on PM_{2.5} mass concentrations from quartz filters and nearby monitoring station.

Date	Urban site ($\mu\text{g}/\text{m}^3$)	Nearby monitoring station ($\mu\text{g}/\text{m}^3$)	Deviation
10/31 DT	69	59	14%
10/31 NT	115	104	10%
11/1 DT	108	94	13%
11/1 NT	75	65	13%
11/2 DT	100	91	9%
11/2 NT	107	96	10%
11/3 DT	110	98	11%
11/3 NT	144	132	8%
11/4 DT	154	141	8%
11/4 NT	228	211	7%
11/5 DT	253	232	8%

-
5. Line 259-261: the haze type was not only defined by the wind direction. In addition to the regional transport, changes in emissions and secondary formation play important roles. For example, biomass burning emissions can increase PM_{2.5} rapidly.

Reply: Based on reviewer's comment, we deleted this sentence.

6. Line 273: what is the major difference for the chemical composition in type 1 and 2.

Reply: The concentrations of OM, K⁺, and secondary inorganic ions were mainly different during the Haze-I and Haze-II events. We showed it in the third paragraph of section 3.1.

P12-13 L295-300: “From the heavy Haze-I to the Haze-II events, secondary inorganic ions significantly decreased from 62-66% of the total PM_{2.5} mass (94-101 µg/m³) to 31-35% (65-70 µg/m³); but OM markedly increased from 27-30% (42-45 µg/m³) to 53-60% (98-133 µg/m³) (Figures 2a-c). In addition, K⁺ average concentrations unexpectedly increased from 1.4 µg/m³ during the heavy Haze-I event to 3.8 µg/m³ during the Haze-II event (Figures 2b-c).”

7. Line 361: so what is the reason of this accumulation?

Reply: The occurrence of stable weather condition (e.g., low wind speed, low pressure, and high RH) led to the accumulation. We added the explanations in the sentence.

P11 L265-269: “Wind, RH, and pressure changed from northerly winds with 1.4 m/s and 4.5 m/s, 35% and 40%, and 1034 hPa and 1002 hPa at the urban and mountain sites on the clean day to southerly winds with 0.7 m/s and 3.0 m/s, 39% and 67%, and 1022 hPa and 991 hPa during the moderate Haze-I event, causing the occurrence of stable meteorological condition (Figures S4a-f).”

P15 L370-372: “This result shows that accumulation of air pollutants under stable meteorological conditions (Figures S4a-f) mainly induced the moderate Haze-I formation.”

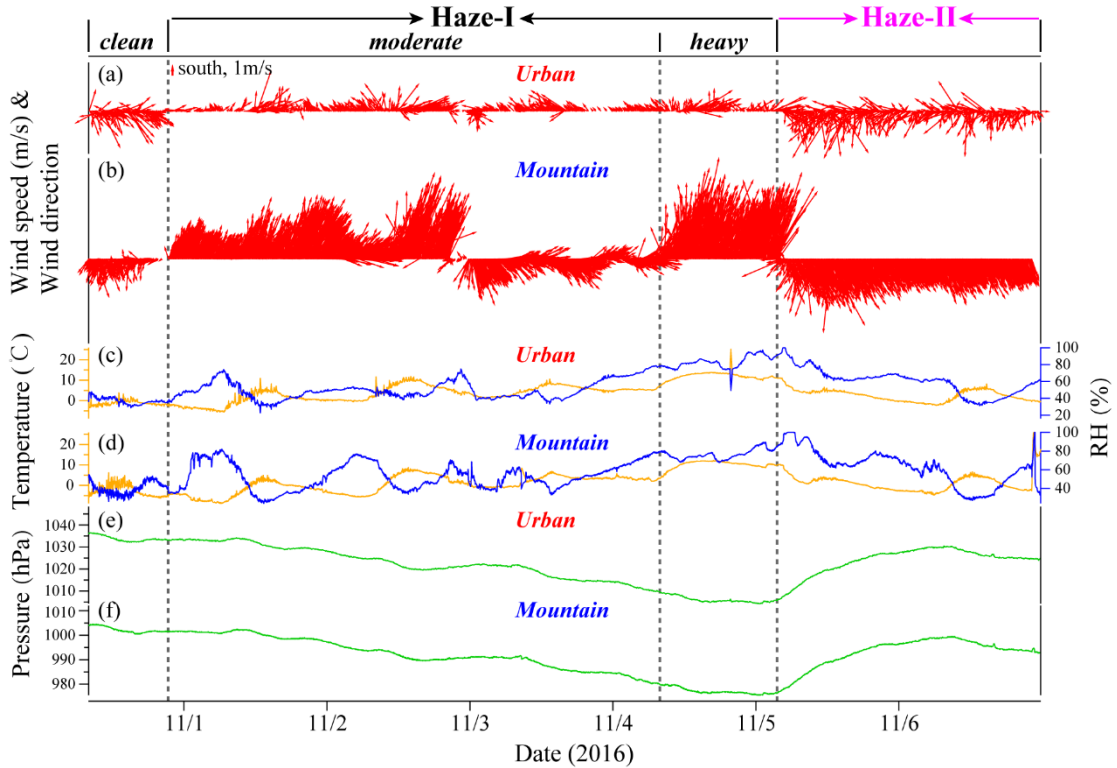


Figure S4. Time series of meteorological parameters at the urban and mountain sites from 31 October to 6 November 2016: (a-b) wind speed and wind direction; (c-d) temperature and relative humidity (RH); (e-f) pressure.

8. Lines 365-367: are those secondary components formed locally or transported the sampling site?

Reply: These secondary components were mainly from local production via heterogeneous reactions and only small part might from transport of Beijing-Tianjin-Hebei region. We added three figures in Figures S5b-d to indicate the geographic origins of haze pollutants. We also added O₃ concentrations in Figure S6d, which showed quite low levels of O₃ during the heavy Haze-I event, indicating that photochemical activity was weak. Moreover, we added some marks in Figure 6 to indicate the phases and mixing states of haze particles. These results suggest the main sources of secondary components. We revised the sentence and explained the main sources of these secondary components in section 4.1.

P15 L375-378: “Figures 5a-b show that SO₄²⁻/EC and NO₃⁻/EC factors reached their maximum values at the two sampling sites during the heavy Haze-I event, suggesting

that secondary sulfates and nitrates significantly increased during Haze-I evolution (details in Section 4.1)."

P17 L434-438: "The significant increases of $\text{SO}_4^{2-}/\text{EC}$, NO_3^-/EC , and $\text{PM}_{2.5}/\text{EC}$ factors from the moderate to heavy Haze-I event (Figures 5a-b) suggest that massive secondary production of sulfates and nitrates elevated $\text{PM}_{2.5}$ concentrations. Figures S5c-d further indicate that compared with transport from Beijing-Tianjin-Hebei region, local secondary transformation was one major factor to cause the heavy Haze-I formation."

P18 L441-449: "Because of low O_3 level at 12 ppb (Figure S6d) and thick haze layer weakening solar radiation (Zhao et al., 2013; Zheng et al., 2015) during the heavy Haze-I event, photochemical activity should be ignored in air and heterogeneous chemical reactions on particle surfaces can be considered as major pathways in the formation of sulfates and nitrates from SO_2 and NO_x whenever RH exceeds 70% (Sun et al., 2018; Wang et al., 2016a; Wu et al., 2018). Here, TEM observations did show that the heavy Haze-I particles were wet aerosols and presented S-rich coating on primary OM, soot, or fly ash/metal particles at 73-80% of RH (Figures 6c-d and S4c-d)."

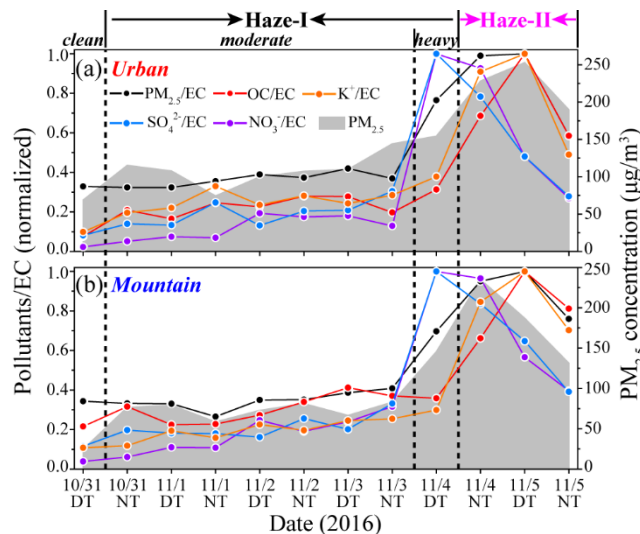


Figure 5. Variation in $\text{PM}_{2.5}/\text{EC}$, OC/EC , $\text{SO}_4^{2-}/\text{EC}$, NO_3^-/EC , and K^+/EC factors at the urban site (a) and mountain site (b). These factors are normalized.

9. Line 371: what is the reason for such a conversion?

Reply: Long-range transport of agricultural biomass burning from the North of

Northeast China induced the conversion from the Haze-I to Haze-II events. Our experimental data are consistent with the changes of meteorological conditions. We revised the sentence and detailedly discussed the cause of conversion in section 4.1.

P15-16 L381-383: “This result indicates that large amounts of aerosol including OM and K⁺ contributed to the conversion from the Haze-I to the Haze-II events (details in Section 4.1).”

P18-19 L460-481: “High levels of K⁺ or K-OM particles represent the influences of biomass burning (Bi et al., 2011; Liu et al., 2017). Indeed, MODIS data during the Haze-II event show that many fire spots occurred in the north part of Northeast China, far away ~580 km from sampling sites, and the air mass backward trajectories at the urban and mountain sites both crossed these fire spots (Figure 7d). MODIS maps further show that these fire spots were in the farming lands instead of the forest areas (Figure 7d). Based on the MODIS data and reports from the local department of ecology and environment (<http://www.hljdep.gov.cn/hjgl/zfjc/jphz/2017/05/15698.html>), these dense fire spots on 4 November were agricultural biomass burning. Open agricultural biomass burning is normally intense during the early winter in Northeast China, a region with abundant agricultural production, because large amounts of agricultural waste need to be cleaned up and their burnt products can be used as fertilizers to increase soil fertility (Cao et al., 2017; Yang et al., 2017). Along with the backward trajectories of air masses, we found sharp PM_{2.5} concentrations occurring from Harbin city (1281 µg/m³ at 18:00 on 4 November) to Changchun city (658 µg/m³ at 0:00 on 5 November) and to Shenyang city (669 µg/m³ at 8:00 on 5 November) (Figure S6a). These above analyses well indicated that long-range transport of agricultural biomass burning emissions directly led to the Haze-II formation (Figure 8) and explained why K⁺/EC, OC/EC, and PM_{2.5}/EC factors together reached their maximum values during the Haze-II event (Figures 5a-b) and K-OM fractions and PM_{2.5} mass concentrations had strong positive correlation (Figure 7b).”

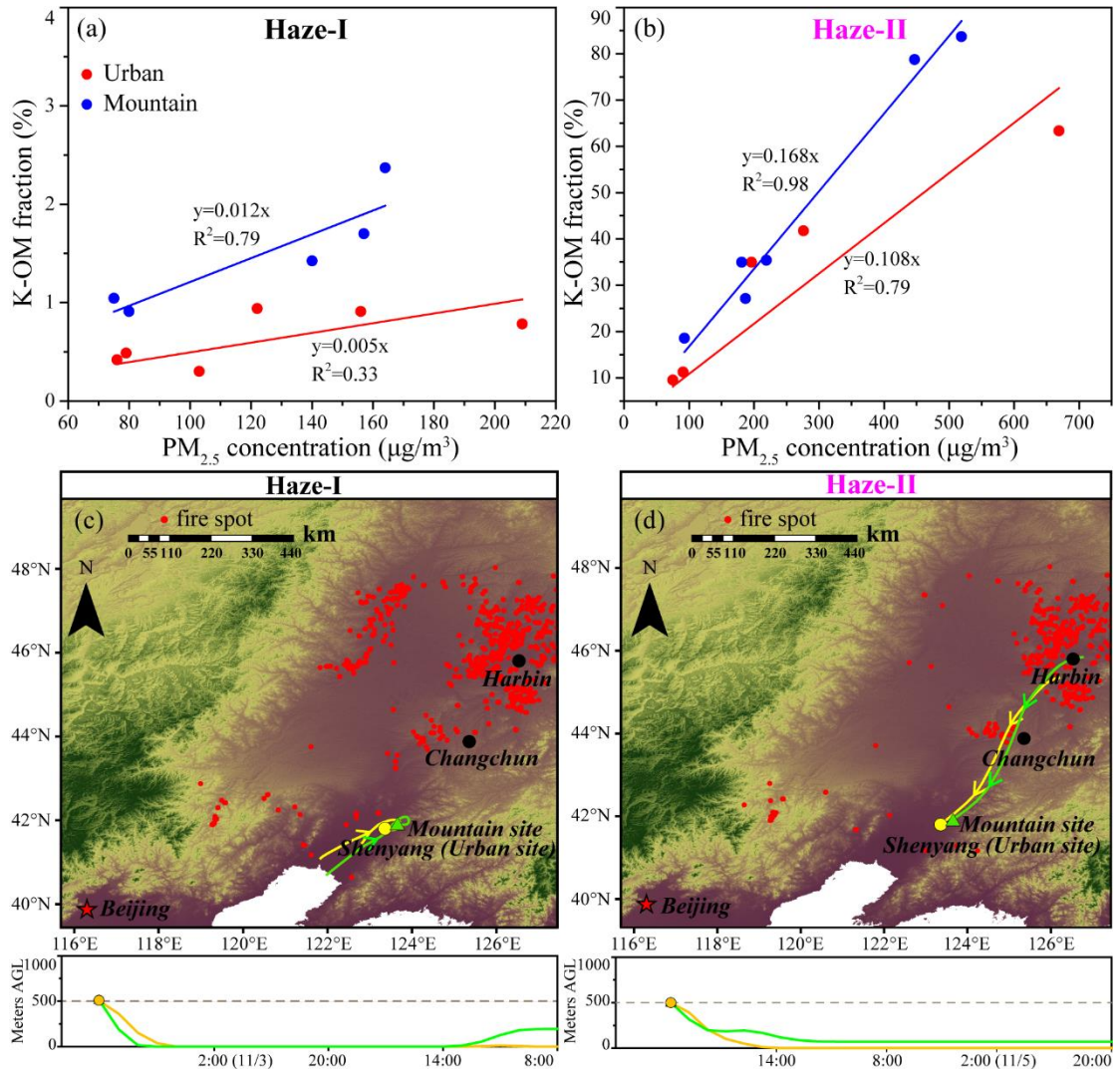


Figure 7. Linear correlations between PM_{2.5} mass concentration (x) and K-OM number fraction (y) during the Haze-I (a) and Haze-II (b). Typical 24-h air mass backward trajectories before arriving at the urban and mountain sites during the Haze-I (c) and Haze-II (d). Fire spot data are from the MODIS Collection 6 Active Fire Product provided by the NASA FIRMS (<https://firms.modaps.eosdis.nasa.gov/map/>).

10. Lines 393-394: how to exclude other emission sources?

Reply: We compared chemical components of Haze-I and Haze-II particles with summertime haze particles that were mainly emitted from industries, coal-fired power plants, and vehicle exhausts. These differences are helpful to exclude the main emission sources such as industries, coal-fired power plants, and vehicle exhausts during the Haze-I and Haze-II events.

P16 L401-407: “TEM observations showed two major types of OM particles during the Haze-I event: spherical OM and domelike OM (Figures 6c-d), which were not frequently observed during summer haze events influenced by industries, coal-fired power plants, and vehicle exhausts (Li et al., 2016; Yuan et al., 2015). Therefore, large numbers of spherical OM and domelike OM particles had no possible from the emissions of industry, coal-fired power plant, and vehicle exhaust.”

11. Line 395: coal combustion may emit K-OM particles.

Reply: We revised the discussion and compared mass concentrations of K^+ and number fractions of K-OM particles during the Haze-I event and haze events influenced by biomass burning to exclude the contribution of biomass burning to Haze-I formation.

P16-17 L410-418: “Many studies found that many haze events caused by biomass burning contained high levels of K^+ at 2.8-5.8 $\mu\text{g}/\text{m}^3$ (Cao et al., 2016; Cheng et al., 2013; Huang et al., 2012; Li et al., 2010a) and K-OM particles at 10-60% by number (Li et al., 2010b; Pósfai et al., 2003; Wang et al., 2016b). However, our results showed quite low K^+ concentration at 1.1 $\mu\text{g}/\text{m}^3$ (Figures 2b-c) and only 3% K-OM (Figure 4) as well as poor correlations with K-OM fractions and $\text{PM}_{2.5}$ concentrations (Figure 7a) during the Haze-I event. The results suggest that biomass burning was not one major source during the Haze-I event. Therefore, we can exclude biomass burning and conclude that coal burning was the major emission source during the Haze-I event.”

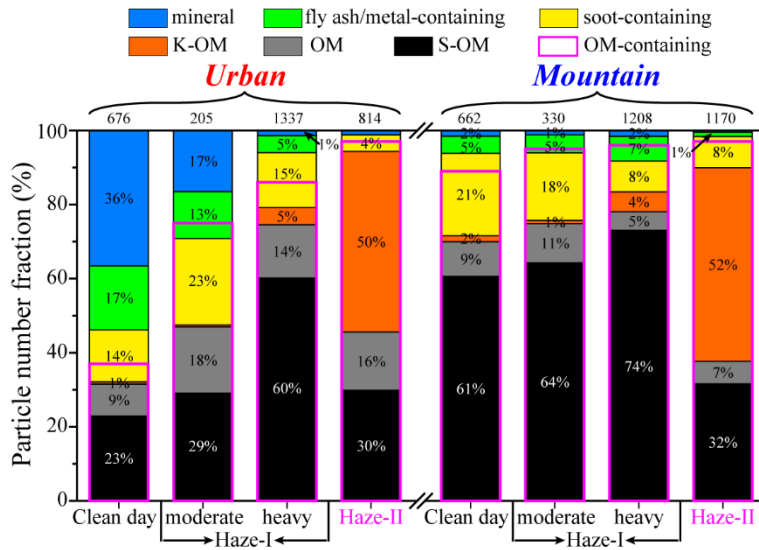


Figure 4. Variation in number fractions of different types of particles at the urban and mountain sites. Analyzed particle numbers are listed on the top of each rectangle.

12. Lines 398-399: no direct evidence. How to exclude other sources, e.g., dust, soil, traffic, secondary formation?

Reply: Please see our reply in Q10. We further compared mass concentrations of K^+ and number fractions of K-OM particles during the Haze-I event and haze events influenced by biomass burning to exclude the contribution of biomass burning to Haze-I formation. The detailed discussion as follows.

P16-17 L401-418: “TEM observations showed two major types of OM particles during the Haze-I event: spherical OM and domelike OM (Figures 6c-d), which were not frequently observed during summer haze events influenced by industries, coal-fired power plants, and vehicle exhausts (Li et al., 2016; Yuan et al., 2015). Therefore, large numbers of spherical OM and domelike OM particles had no possible from the emissions of industry, coal-fired power plant, and vehicle exhaust. Moreover, the similar OM particles have been considered as primary OM aerosols and they can be directly emitted from residential coal burning (Zhang et al., 2018) or biomass burning (Liu et al., 2017). Many studies found that many haze events caused by biomass burning contained high levels of K^+ at $2.8\text{-}5.8 \mu\text{g}/\text{m}^3$ (Cao et al., 2016; Cheng et al., 2013; Huang et al., 2012; Li et al., 2010a) and K-OM particles at 10-60% by number (Li et al., 2010b; Pósfai et al.,

2003; Wang et al., 2016b). However, our results showed quite low K⁺ concentration at 1.1 µg/m³ (Figures 2b-c) and only 3% K-OM (Figure 4) as well as poor correlations with K-OM fractions and PM_{2.5} concentrations (Figure 7a) during the Haze-I event. The results suggest that biomass burning was not one major source during the Haze-I event. Therefore, we can exclude biomass burning and conclude that coal burning was the major emission source during the Haze-I event.”

13. Lines 409-410: what is the direct evidence?

Reply: Heating activities in Northeast China during winter are abundant because of very low temperature. The previous studies have suggested that although central heating is carried out in urban areas in Northeast China, large numbers of residential stoves without emission controls are used for household heating and cooking through burning coals in the rural and suburban areas that do emit abundant primary OM particles. We further analyzed meteorological data (Figures S4a-b), air mass backward trajectory (Figure 7c), and concentration-weighted trajectory (CWT) plots of PM_{2.5} (Figures S5b-d) during the Haze-I event, concluding that large numbers of primary OM particles during the Haze-I event were mainly from regional emissions of coal burning in residential stoves for heating and cooking. The detailed discussion as follows.

P17 L419-433: “During the wintertime with the lowest temperature at about -30 °C in Northeast China, high-intensity coal burning activities for household heating are necessary (Yang et al., 2017; Zhang et al., 2017). Central heating via large boilers equipped with efficient filters are in wide use in the urban areas in Northeast China, but large numbers of residential stoves without emission controls are still used for household heating and cooking through burning coals in the rural and suburban areas that do emit abundant primary OM particles (Xu et al., 2017; Zhang et al., 2017). Through the meteorological data (Figures S4a-b), air mass backward trajectory (Figure 7c), and concentration-weighted trajectory (CWT) plots of PM_{2.5} (Figures S5b-d) analyses, we inferred that the air quality at the two sampling sites during the Haze-I event was mostly influenced by Shenyang city and its nearby surrounding emissions, although transport from Beijing-Tianjin-Hebei region slightly contributed to the heavy

Haze-I formation on 4 DT November. In a word, we determined that large amounts of fine primary OM aerosol during the Haze-I event were mainly from regional emissions of coal burning in residential stoves for heating and cooking as shown in Figure 8.”

14. Lines: 427-429: the evidence of heterogeneous reactions should be provided; otherwise it is too speculative.

Reply: We added O₃ concentrations in Figure S6d, which showed quite low levels of O₃ during the heavy Haze-I event, indicating that photochemical activity was extremely weak. Moreover, we added some marks in Figure 6 to indicate the phases and mixing states of haze particles. These results well contributed to prove heterogeneous reactions.

The detailed discussion as follows.

P18 L441-451: “Because of low O₃ level at 12 ppb (Figure S6d) and thick haze layer weakening solar radiation (Zhao et al., 2013; Zheng et al., 2015) during the heavy Haze-I event, photochemical activity should be ignored in air and heterogeneous chemical reactions on particle surfaces can be considered as major pathways in the formation of sulfates and nitrates from SO₂ and NO_x whenever RH exceeds 70% (Sun et al., 2018; Wang et al., 2016a; Wu et al., 2018). Here, TEM observations did show that the heavy Haze-I particles were wet aerosols and presented S-rich coating on primary OM, soot, or fly ash/metal particles at 73-80% of RH (Figures 6c-d and S4c-d). Obviously, the preexisting particles in the hazes provided large heterogeneous surfaces for the formation of sulfates and nitrates (He et al., 2014; Li et al., 2011; Wang et al., 2016a).”

References

- Bi, X., Zhang, G., Li, L., Wang, X., Li, M., Sheng, G., Fu, J., and Zhou, Z.: Mixing state of biomass burning particles by single particle aerosol mass spectrometer in the urban area of PRD, China, *Atmos. Environ.*, 45, 3447-3453, <https://doi.org/10.1016/j.atmosenv.2011.03.034>, 2011.
- Cao, F., Zhang, S. C., Kawamura, K., and Zhang, Y. L.: Inorganic markers, carbonaceous components and stable carbon isotope from biomass burning aerosols in Northeast China, *The Science of the total environment*, 572, 1244-1251, <https://doi.org/10.1016/j.scitotenv.2015.09.099>, 2016.
- Cao, F., Zhang, S. C., Kawamura, K., Liu, X., Yang, C., Xu, Z., Fan, M., Zhang, W., Bao, M., Chang, Y., Song, W., Liu, S., Lee, X., Li, J., Zhang, G., and Zhang, Y. L.: Chemical characteristics of dicarboxylic acids and related organic compounds in PM_{2.5} during biomass-burning and non-biomass-burning seasons at a rural site of Northeast China, *Environ. Pollut.*, 231, 654-662, <https://doi.org/10.1016/j.envpol.2017.08.045>, 2017.
- Cheng, Y., Engling, G., He, K. B., Duan, F. K., Ma, Y. L., Du, Z. Y., Liu, J. M., Zheng, M., and Weber, R. J.: Biomass burning contribution to Beijing aerosol, *Atmospheric Chemistry and Physics*, 13, 7765-7781, <https://doi.org/10.5194/acp-13-7765-2013>, 2013.
- He, H., Wang, Y., Ma, Q., Ma, J., Chu, B., Ji, D., Tang, G., Liu, C., Zhang, H., and Hao, J.: Mineral dust and NO_x promote the conversion of SO₂ to sulfate in heavy pollution days, *Sci. Rep.*, 4, 4172, <https://doi.org/10.1038/srep04172>, 2014.
- Huang, K., Zhuang, G., Lin, Y., Fu, J. S., Wang, Q., Liu, T., Zhang, R., Jiang, Y., Deng, C., Fu, Q., Hsu, N. C., and Cao, B.: Typical types and formation mechanisms of haze in an Eastern Asia megacity, Shanghai, *Atmospheric Chemistry and Physics*, 12, 105-124, <https://doi.org/10.5194/acp-12-105-2012>, 2012.
- Li, H., Han, Z., Cheng, T., Du, H., Kong, L., Chen, J., Zhang, R., and Wang, W.: Agricultural Fire Impacts on the Air Quality of Shanghai during Summer Harvesttime, *Aerosol and Air Quality Research*, 10, 95-101, <https://doi.org/10.4209/aaqr.2009.08.0049>, 2010a.
- Li, W., Zhou, S., Wang, X., Xu, Z., Yuan, C., Yu, Y., Zhang, Q., and Wang, W.: Integrated evaluation of aerosols from regional brown hazes over northern China in winter: Concentrations, sources, transformation, and mixing states, *J. Geophys. Res.*, 116, D09301, <https://doi.org/10.1029/2010JD015099>, 2011.
- Li, W., Sun, J., Xu, L., Shi, Z., Riemer, N., Sun, Y., Fu, P., Zhang, J., Lin, Y., Wang, X., Shao, L., Chen, J., Zhang, X., Wang, Z., and Wang, W.: A conceptual framework for mixing structures in individual aerosol particles, *J. Geophys. Res.-Atmos.*, 121, 13784-13798, <https://doi.org/10.1002/2016JD025252>, 2016.
- Li, W. J., Shao, L. Y., and Buseck, P. R.: Haze types in Beijing and the influence of agricultural biomass burning, *Atmospheric Chemistry and Physics*, 10, 8119-8130, <https://doi.org/10.5194/acp-10-8119-2010>, 2010b.
- Liu, L., Kong, S., Zhang, Y., Wang, Y., Xu, L., Yan, Q., Lingaswamy, A. P., Shi, Z., Lv, S., Niu, H., Shao, L., Hu, M., Zhang, D., Chen, J., Zhang, X., and Li, W.: Morphology, composition, and mixing state of primary particles from combustion sources-crop residue, wood, and solid waste, *Sci. Rep.*, 7, 5047, <https://doi.org/10.1038/s41598-017-05357-2>, 2017.
- Pósfai, M., Simonics, R., Li, J., Hobbs, P. V., and Buseck, P. R.: Individual aerosol particles from biomass burning in southern Africa: 1. Compositions and size distributions of carbonaceous particles, *J. Geophys. Res.-Atmos.*, 108, D138483, <https://doi.org/doi:10.1029/2002jd002291>, 2003.
- Sun, J., Liu, L., Xu, L., Wang, Y., Wu, Z., Hu, M., Shi, Z., Li, Y., Zhang, X., Chen, J., and Li, W.: Key

Role of Nitrate in Phase Transitions of Urban Particles: Implications of Important Reactive Surfaces for Secondary Aerosol Formation, J. Geophys. Res.-Atmos., 123, 1234-1243, <https://doi.org/10.1002/2017JD027264>, 2018.

Wang, G., Zhang, R., Gomez, M. E., Yang, L., Levy Zamora, M., Hu, M., Lin, Y., Peng, J., Guo, S., Meng, J., Li, J., Cheng, C., Hu, T., Ren, Y., Wang, Y., Gao, J., Cao, J., An, Z., Zhou, W., Li, G., Wang, J., Tian, P., Marrero-Ortiz, W., Secretst, J., Du, Z., Zheng, J., Shang, D., Zeng, L., Shao, M., Wang, W., Huang, Y., Wang, Y., Zhu, Y., Li, Y., Hu, J., Pan, B., Cai, L., Cheng, Y., Ji, Y., Zhang, F., Rosenfeld, D., Liss, P. S., Duce, R. A., Kolb, C. E., and Molina, M. J.: Persistent sulfate formation from London Fog to Chinese haze, P. Natl. Acad. Sci. USA, 113, 13630-13635, <https://doi.org/10.1073/pnas.1616540113>, 2016a.

Wang, H., An, J., Shen, L., Zhu, B., Xia, L., Duan, Q., and Zou, J.: Mixing state of ambient aerosols in Nanjing city by single particle mass spectrometry, Atmos. Environ., 132, 123-132, <https://doi.org/10.1016/j.atmosenv.2016.02.032>, 2016b.

Wu, Z., Wang, Y., Tan, T., Zhu, Y., Li, M., Shang, D., Wang, H., Lu, K., Guo, S., Zeng, L., and Zhang, Y.: Aerosol Liquid Water Driven by Anthropogenic Inorganic Salts: Implying Its Key Role in Haze Formation over the North China Plain, Environ. Sci. Technol. Lett., 5, 160-166, <https://doi.org/10.1021/acs.estlett.8b00021>, 2018.

Xu, L., Liu, L., Zhang, J., Zhang, Y., Ren, Y., Wang, X., and Li, W.: Morphology, Composition, and Mixing State of Individual Aerosol Particles in Northeast China during Wintertime, Atmosphere, 8, 47-57, <https://doi.org/10.3390/atmos8030047>, 2017.

Yang, T., Gbaguidi, A., Yan, P., Zhang, W., Zhu, L., Yao, X., Wang, Z., and Chen, H.: Model elucidating the sources and formation mechanisms of severe haze pollution over Northeast mega-city cluster in China, Environ. Pollut., 230, 692-700, <https://doi.org/10.1016/j.envpol.2017.06.007>, 2017.

Yuan, Q., Li, W., Zhou, S., Yang, L., Chi, J., Sui, X., and Wang, W.: Integrated evaluation of aerosols during haze-fog episodes at one regional background site in North China Plain, Atmos. Res., 156, 102-110, <https://doi.org/doi:10.1016/j.atmosres.2015.01.002>, 2015.

Zhang, J., Liu, L., Wang, Y., Ren, Y., Wang, X., Shi, Z., Zhang, D., Che, H., Zhao, H., Liu, Y., Niu, H., Chen, J., Zhang, X., Lingaswamy, A. P., Wang, Z., and Li, W.: Chemical composition, source, and process of urban aerosols during winter haze formation in Northeast China, Environ. Pollut., 231, 357-366, <https://doi.org/10.1016/j.envpol.2017.07.102>, 2017.

Zhang, Y., Yuan, Q., Huang, D., Kong, S., Zhang, J., Wang, X., Lu, C., Shi, Z., Zhang, X., and Sun, Y.: Direct observations of fine primary particles from residential coal burning: insights into their morphology, composition, and hygroscopicity, J. Geophys. Res.-Atmos., 123, 12964-12979, <https://doi.org/10.1029/2018JD028988>, 2018.

Zhao, X. J., Zhao, P. S., Xu, J., Meng, W., Pu, W. W., Dong, F., He, D., and Shi, Q. F.: Analysis of a winter regional haze event and its formation mechanism in the North China Plain, Atmos. Chem. Phys., 13, 5685-5696, <https://doi.org/10.5194/acp-13-5685-2013>, 2013.

Zheng, G. J., Duan, F. K., Su, H., Ma, Y. L., Cheng, Y., Zheng, B., Zhang, Q., Huang, T., Kimoto, T., Chang, D., Pöschl, U., Cheng, Y. F., and He, K. B.: Exploring the severe winter haze in Beijing: the impact of synoptic weather, regional transport and heterogeneous reactions, Atmos. Chem. Phys., 15, 2969-2983, <https://doi.org/10.5194/acp-15-2969-2015>, 2015.

Zhong, J., Zhang, X., Wang, Y., Wang, J., Shen, X., Zhang, H., Wang, T., Xie, Z., Liu, C., Zhang, H., Zhao, T., Sun, J., Fan, S., Gao, Z., Li, Y., and Wang, L.: The two-way feedback mechanism between unfavorable meteorological conditions and cumulative aerosol pollution in various haze regions of

